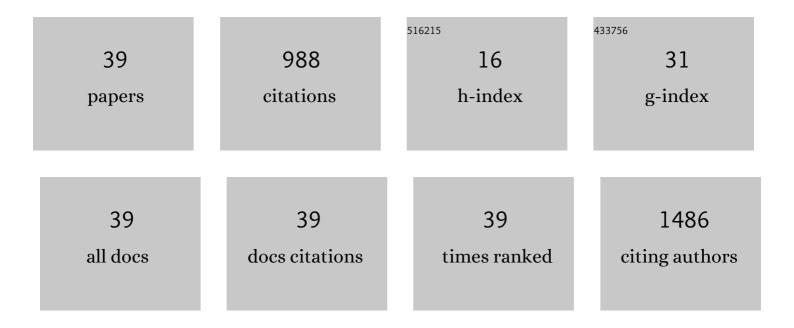
## Wen-Zhu Shao

List of Publications by Year in descending order

Source: https://exaly.com/author-pdf/9068815/publications.pdf Version: 2024-02-01



**Μενη-ΖΗΠ SHAO** 

#	Article	IF	CITATIONS
1	Effects of interfacial wettability on arc erosion behavior of Zn2SnO4/Cu electrical contacts. Journal of Materials Science and Technology, 2022, 109, 64-75.	5.6	17
2	Microstructures and Magnetic Properties of Single-Step Deposited Ce:YIG/YIG Bilayer Films With Different Layer Thickness Ratios. IEEE Transactions on Magnetics, 2022, 58, 1-5.	1.2	0
3	Effect of Pre-Stretch on the Precipitation Behavior and the Mechanical Properties of 2219 Al Alloy. Materials, 2021, 14, 2101.	1.3	3
4	Precipitation during Quenching in 2A97 Aluminum Alloy and the Influences from Grain Structure. Materials, 2021, 14, 2802.	1.3	2
5	Tuning the Energy Storage Efficiency in PVDF Nanocomposites Incorporated with Crumpled Core–Shell BaTiO <sub>3</sub> @Graphene Oxide Nanoparticles. ACS Applied Energy Materials, 2021, 4, 9553-9562.	2.5	12
6	Texture evolution and recrystallization mechanism in a Mg–3Al–1Zn alloy under ballistic impact. Journal of Alloys and Compounds, 2020, 816, 152599.	2.8	11
7	Highly localized shear deformation in a Mg–Al–Mn alloy subjected to ballistic impact. Vacuum, 2019, 169, 108868.	1.6	13
8	Adhesion and electronic structures of Cu/Zn2SnO4 interfaces: A first-principles study. Journal of Applied Physics, 2019, 125, .	1.1	6
9	The effect of Cu and Sc on the localized corrosion resistance of Al-Zn-Mg-X alloys. Journal of Alloys and Compounds, 2019, 799, 1-14.	2.8	63
10	Hybrid dual-channel phototransistor based on 1D t-Se and 2D ReS2 mixed-dimensional heterostructures. Nano Research, 2019, 12, 669-674.	5.8	34
11	Enhancement of strength and electrical conductivity for a dilute Al-Sc-Zr alloy via heat treatments and cold drawing. Journal of Materials Science and Technology, 2019, 35, 962-971.	5.6	56
12	Electron structure in modified BaTiO <sub>3</sub> /poly(vinylidene fluoride) nanocomposite with high dielectric property and energy density. IET Nanodielectrics, 2019, 2, 70-77.	2.0	14
13	Air arc erosion behavior of CuZr/Zn2SnO4 electrical contact materials. Journal of Alloys and Compounds, 2018, 743, 697-706.	2.8	16
14	Effects of dopants on the adhesion and electronic structure of a SnO <sub>2</sub> /Cu interface: a first-principles study. Physical Chemistry Chemical Physics, 2018, 20, 15618-15625.	1.3	11
15	Epitaxial Growth of 1D Atomic Chain Based Se Nanoplates on Monolayer ReS <sub>2</sub> for Highâ€Performance Photodetectors. Advanced Functional Materials, 2018, 28, 1806254.	7.8	52
16	Surface characterization and degradation behavior of polyimide films induced by coupling irradiation treatment. RSC Advances, 2018, 8, 28152-28160.	1.7	28
17	Microstructure evolution of polyimide films induced by electron beam irradiation-load coupling treatment. Polymer Degradation and Stability, 2018, 155, 230-237.	2.7	11
18	Microstructure Evolution and the Resulted Influence on Localized Corrosion in Al-Zn-Mg-Cu Alloy during Non-Isothermal Ageing. Materials, 2018, 11, 720.	1.3	17

Wen-Zhu Shao

#	Article	IF	CITATIONS
19	Chemical Vapor Deposition Growth of Degenerate p-Type Mo-Doped ReS <sub>2</sub> Films and Their Homojunction. ACS Applied Materials & Interfaces, 2017, 9, 15583-15591.	4.0	30
20	van der Waals epitaxy of large-area continuous ReS <sub>2</sub> films on mica substrate. RSC Advances, 2017, 7, 24188-24194.	1.7	29
21	Thermal conductivity determination of conductor/insulator composites by fractal: Geometrical tortuosity and percolation. Composites Part B: Engineering, 2016, 92, 377-383.	5.9	10
22	Internal Biasing in Relaxor Ferroelectric Polymer to Enhance the Electrocaloric Effect. Advanced Functional Materials, 2015, 25, 5134-5139.	7.8	64
23	Dielectric and electrocaloric responses of Ba(Zr <sub>0.2</sub> Ti <sub>0.8</sub> )O <sub>3</sub> bulk ceramics and thick films with sintering aids. IEEE Transactions on Dielectrics and Electrical Insulation, 2015, 22, 1501-1505.	1.8	15
24	Minimization of Residual Stress in an Al-Cu Alloy Forged Plate by Different Heat Treatments. Journal of Materials Engineering and Performance, 2015, 24, 2256-2265.	1.2	29
25	Exploring Cu2O/Cu cermet as a partially inert anode to produce aluminum in a sustainable way. Journal of Alloys and Compounds, 2014, 610, 214-223.	2.8	11
26	Colloidal synthesis and formation mechanism of calcium molybdate notched microspheres. CrystEngComm, 2014, 16, 2598.	1.3	9
27	Mechanical properties of cermet composites with various geometrical tortuosity of metal phase: Fractal characterization. Materials Science & Engineering A: Structural Materials: Properties, Microstructure and Processing, 2014, 607, 236-244.	2.6	7
28	Effect of electron irradiation on electroactive phase and dielectric properties of PVDF films. RSC Advances, 2014, 4, 13525-13532.	1.7	13
29	Self-supported construction of 3D CdMoO <sub>4</sub> hierarchical structures from nanoplates with enhanced photocatalytic properties. RSC Advances, 2014, 4, 38527-38534.	1.7	7
30	Formation of CdMoO4 porous hollow nanospheres via a self-assembly accompanied with Ostwald ripening process and their photocatalytic performance. CrystEngComm, 2013, 15, 8014.	1.3	39
31	Effect of electroactive phase transformation on electron structure and dielectric properties of uniaxial stretching poly(vinylidene fluoride) films. RSC Advances, 2013, 3, 23730.	1.7	76
32	Crystallization kinetics and phase transformation of poly(vinylidene fluoride) films incorporated with functionalized baTiO <sub>3</sub> nanoparticles. Journal of Applied Polymer Science, 2013, 129, 2940-2949.	1.3	92
33	Fractal Analysis of Disordered Conductor–Insulator Composites with Different Conductor Backbone Structures near Percolation Threshold. Journal of Physical Chemistry C, 2012, 116, 19517-19525.	1.5	24
34	Formation of FeMoO4 hollow microspheres via a chemical conversion-induced Ostwald ripening process. CrystEngComm, 2012, 14, 7025.	1.3	37
35	Synthesis of Fe–ferrite composite nanotubes with excellent microwave absorption performance. CrystEngComm, 2011, 13, 6839.	1.3	40
36	Synthesis and formation process of SrSO <sub>4</sub> sisal-like hierarchical structures at room temperature. CrystEngComm, 2011, 13, 620-625.	1.3	14

Wen-Zhu Shao

#	Article	IF	CITATIONS
37	Deformed Microstructure of AZ91 Magnesium Alloy Impacted by Projectiles with Velocities of 2-3 km/s. Journal of Solid Mechanics and Materials Engineering, 2010, 4, 720-726.	0.5	2
38	Aqueous Solution Synthesis of Cd(OH)2 Hollow Microspheres via Ostwald Ripening and Their Conversion to CdO Hollow Microspheres. Journal of Physical Chemistry C, 2008, 112, 14360-14366.	1.5	62
39	Correlation between Structural Evolution and Device Performance of CH3NH3PbI3 Solar Cells under Proton Irradiation. ACS Applied Energy Materials, 0, , .	2.5	12